

Self-weight Distortion of Lens Elements

Frank DeWitt IV, Georg Nadorff, Markar Naradikian
Melles Griot, 55 Science Parkway, Rochester, NY 14620
phone +1 585 244-7220; email mgoptics@idexcorp.com

COPYRIGHT 2006 Society of Photo-Optical Instrumentation Engineers

This paper was published in Proc. SPIE Vol. 6288, *Current Developments in Lens Design and Optical Engineering VII*, edited by Pantazis Z. Mouroulis, Warren J. Smith, R. Barry Johnson, 62880H (2006)
doi:10.1117/12.679138; <http://dx.doi.org/10.1117/12.679138>

One print or electronic copy may be made for personal use only. Systematic reproduction and distribution, duplication of any material in this paper for a fee or for commercial purposes, or modification of the content of the paper are prohibited.

Self-weight Distortion of Lens Elements

Frank DeWitt IV, Georg Nadorff, Markar Naradikian
Melles Griot Optics Group, 55 Science Parkway, Rochester, NY 14620

ABSTRACT

Changes in the shape of large lens elements due to the influences of gravity are important to consider in the fabrication, testing and assembly of optical systems. Tried and proven methods used for mounting large mirrors to minimize the effects of gravity are typically not applicable to large transmissive lens elements, due to the simple requirement that the clear aperture of a lens must remain free of mechanical obstructions. Precautions must be taken to ensure that an element's surfaces are correctly fabricated and then maintained when assembled into the final system. The amount of distortion caused by the weight of a particular lens element is dependent on a number of factors including: size, aspect ratio, shape, material, and the support on which it rests. Examples of the effects of these factors are modeled using Finite Element Analysis and demonstrated through interferometric testing. Attention is given to the mounting of lens elements within a system and simulating "real-world" conditions. These "real-world" conditions can produce results that are different from what was expected if only ideal cases have been considered. The work presented will aid the designer, fabricator, and metrologist to identify what optical elements and mounting conditions may be problematic and to minimize their effects.

Keywords: optomechanical, finite element analysis, self-weight distortion, gravity, sag, optical mounting, tolerancing, surface irregularity

1. INTRODUCTION

Self-weight distortion is not a new problem to the opto-mechanical engineer, lens designer or metrologist, but the reality of the constant push for higher performance in smaller packages has led to increased challenges. Self-weight distortion of optical elements is most pronounced on large optics and, therefore, much of the effort in both understanding and controlling it has been targeted toward large telescope primary mirrors. However, as the requirements for surface irregularities have steadily become more stringent, driven in part by the decreasing operational wavelengths of optical lithography tools, issues with self-weight deflection have begun to affect elements of only a few inches in diameter. Often, imperfect lens seats and other "real world" conditions may amplify distortions due to gravity over what might otherwise have been expected.

We begin by providing a methodology to determine the sag due to gravity of a horizontally mounted plane cylindrical plate. The developed formulae provide insight into the factors that affect the magnitude of the self-weight deflection for specific optical lens elements. Using Finite Element Analysis (FEA), we then examine the influence of lens shape on the amount of deflection we would anticipate and compare with the closed-form solution. Results from the analysis and interferometric metrology of "real world" cases are discussed, including causes for departure from the ideal predicted models.

2. SELF-WEIGHT DISTORTION OF AN EDGE SUPPORTED CYLINDRICAL PLATE

We desire to determine the effects of part scale, part thickness, and specific stiffness on the gravity sag of an optical element. Consider a circular plane parallel plate of uniform thickness supported at its edge. The analogous real-world situation would be a optical window sitting freely on a compliant ring¹ near the outermost edge. Gravity will have the greatest effect on the sag of the window when the window is oriented in a horizontal position such that gravity is "pulling the center down." This case is shown in cross-section in Figure 1.

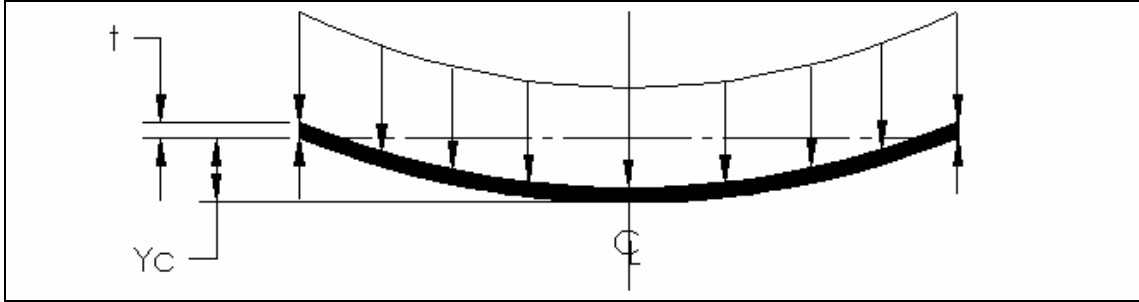


Figure 1: Simply supported disk with uniform pressure load

The closed-form solutions found in “Roarks Formulas for Stress and Strain”² are useful for demonstrating the effects of part scale, part thickness, and specific stiffness. If the “plate constant,” D , is given by:

$$D = \frac{E \cdot t^3}{12(1 - \nu^2)} \quad (1)$$

where t = plate thickness, ν = Poisson’s ratio, and E = Young’s modulus of elasticity, then the deflection, y_c , of the uniform disk with an applied uniform pressure load (in our case the weight of the disk itself) is given by:

$$y_c = \frac{-q \cdot a^4 (5 + \nu)}{64D(1 + \nu)} \quad (2)$$

where a = radius of the plate, and q = load per unit area given by:

$$q = \rho \cdot t \cdot g \quad (3)$$

where ρ = material density and g = acceleration due to gravity.

We can now explore the effects of part thickness, part scale, and specific density (the ratio of E/ρ) on the self-weight deflection of a circular plate. For purposes of illustration, let us consider a window made of Schott F5 optical glass ($\nu = 0.22$, $E = 58 \times 10^9$ Pa, $\rho = 3470$ kg/m³). It has an aspect ratio (the ratio of the lens’ diameter to its center thickness) of 8:1, with a diameter of 4 inches and a thickness of 0.5 inches. If we independently vary in turn the thickness, specific density, and part scale from 0.5x to 2x the original values, as shown in Table 1,

Scale Factor	0.5x	1x	2x
Varying Thickness	Diameter: 4.0" Thickness: 0.25" E/ ρ : 16.7	Diameter: 4.0" Thickness: 0.50" E/ ρ : 16.7	Diameter: 4.0" Thickness: 1.00" E/ ρ : 16.7
Varying Specific Density	Diameter: 4.0" Thickness: 0.50" E/ρ: 8.35	Diameter: 4.0" Thickness: 0.50" E/ρ: 16.7	Diameter: 4.0" Thickness: 0.50" E/ρ: 33.4
Varying Part Scale	Diameter: 2.0" Thickness: 0.25" E/ ρ : 16.7	Diameter: 4.0" Thickness: 0.50" E/ ρ : 16.7	Diameter: 8.0" Thickness: 1.00" E/ ρ : 16.7

Table 1: Parameters of test cases shown in Figure 2

then plotting y_c (converted to waves at 633 nm) as a function of scale factor yields the relationships plotted in Figure 2.

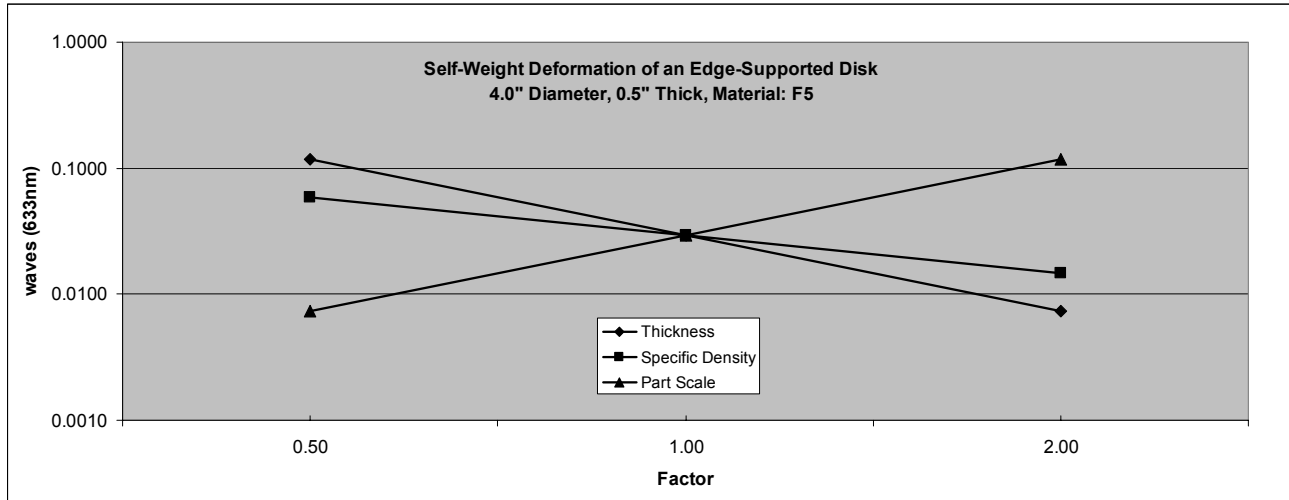


Figure 2: Self-weight deflection of an edge supported disk

As was to be expected, the part thickness has a significant effect on its self-weight deflection. Surprisingly, however, the part *scale* has a similar but opposite effect. Therefore, for our F5 disk, even as the aspect ratio of 8:1 is maintained, if the dimensions are uniformly scaled either up or down, the self-weight deflection is dramatically changed.

While not as severe, specific density also affects the magnitude of self-weight deflection. The broad range of the specific densities of some common optical glasses is shown in Table 2.

Glass Type	Modulus, E (Pa) x 10 ⁹	Density (kg/m ³), ρ x 10 ³	Specific Density, E/ρ x 10 ⁶
BK7	81	2.51	32.27
Fused Silica	67	2.21	30.32
F5	58	3.47	16.71
SF6	56	5.18	10.81

Table 2: Specific density of various glass types³

Depending on what level of sag deformation of an optical element is tolerable, the analysis suggests that element aspect ratios alone are not sufficient to guarantee as-used performance. They should be applied with caution. At minimum, they are only relevant for optics of similar diameters and similar specific densities. Material type and *diameter* must also be considered.

In this regard, the next application of Equations (1) to (3), for a given diameter and material, is to determine the minimum thickness required to achieve a maximum deflection. Historically, optical engineers tend to consider only the aspect ratio as a guide to determine a lens’ minimum center thickness. They have learned from opticians, that the desired lens shape is easier to achieve during fabrication when the aspect ratio is at most 6:1 (5:1 being better, 4:1 better still, and so on). If the lens diameter is pre-determined by the optical requirements for a given optical system, then the lens thickness may simply be assigned (or targeted) using the aspect ratio rule of thumb. However, is the “minimum” aspect ratio of 6:1, while acceptable to the optician, good enough for the as-built optical system to avoid self-weight deflection to a certain level?

Solving Equations (1) to (3) for t , the minimum part thickness to achieve a maximum value of center deflection yields:

$$t = \sqrt{\frac{3\rho \cdot g \cdot a^4 (5 + \nu)(1 - \nu)}{16E \cdot |y_c|}} \quad (4)$$

In optical lithography, for example, typical requirements may dictate that an optical system is to be used in a vertical orientation (parallel to gravity), and that lens element surface accuracies of better than $\lambda/50$ need to be maintained. In this case, $y_c = \lambda/50 = 0.02 \lambda = 12.7 \text{ nm}$ (@ $\lambda = 633 \text{ nm}$). Then for our F5 window, we can use Equation (4) to tabulate the relationship between aspect ratio and part diameter, as in Table 3:

Part Diameter (mm)	Maximum Aspect Ratio
25	35:1
50	17:1
100	9:1
150	6:1
200	4:1

Table 3: Aspect ratio required to prevent self-weight distortions in excess of $\lambda/50$.

We can see that for “small” to “medium” sized optics (less than 6-inch diameter), the 6:1 aspect ratio will work. However, for “large” optics (greater than 6-inch diameter), the 6:1 aspect ratio is not sufficient and the element thicknesses would need to be increased. Another example would be to find the minimum thickness required to produce a transmission flat that, when used in a vertically oriented interferometer, would not sag more than what the reference surface on the flat is guaranteed to be accurate to. Flats of 4-inch and 6-inch diameter are industry standards, with larger flats for custom-built interferometers not uncommon.

3. FEA OF OPTICAL ELEMENTS

Equations (1) to (4) are useful for establishing how part size and material properties affect self-weight deflection, but additional analysis is required to determine how these results relate to actual lens shapes with spherical surfaces. For our purposes, we will consider four different lens shapes: plano-convex, plano-concave, convex-concave (meniscus), and plano-plano, as shown in Figure 3.

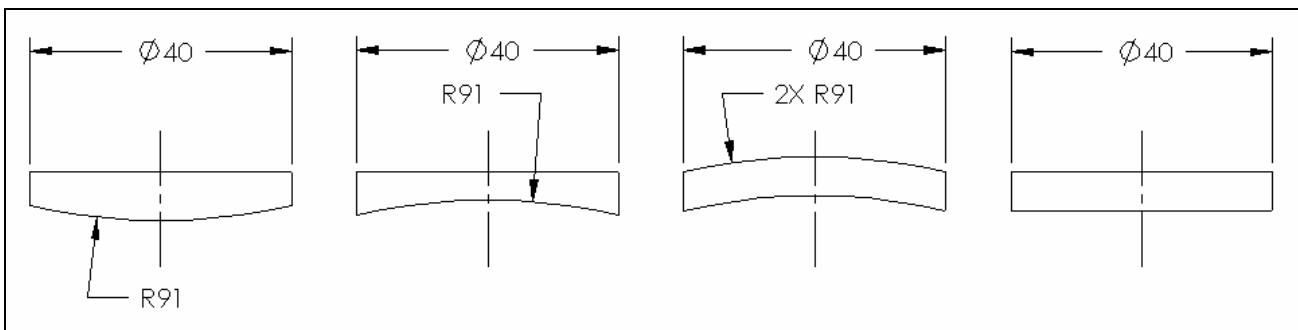


Figure 3: Lens shapes

Using Finite Element Analysis, we will analyze the sensitivities of each of these four lens shapes. Two scenarios are considered. The first maintains a constant average thickness, thus keeping the masses of the four elements similar. The second maintains the center thickness for each shape. The radii and diameters of the elements were arbitrarily chosen to be 91 mm and 40 mm, respectively, and the material was again Schott F5. In all cases, the elements were simply supported on the lower, outer edge of the element: in-plane translation was allowed, but translation normal to the support-plane was constrained. Table 4 tabulates the results of this exercise. Included are columns indicating how closely the lens shape of each case compares to a FEA result for a plano-plano element.

Self Weight Deflection for Varied Lens Shapes, FEA Results				
	Constant Average Thickness Case	% Difference from Average Thickness, PL-PL, FEA Result	Constant Center Thickness Case	% Difference from Average Thickness, PL-PL, FEA Result
PL-CX	5.09 nm	8.45%	5.09 nm	24.75%
PL-CC	7.80 nm	29.23%	2.81 nm	-36.30%
Meniscus	4.33 nm	27.48%	3.36 nm	-13.99%
PL-PL (FEA)	5.52 nm	0.00%	3.83 nm	0.00%
PL-PL (Eq. 2)	5.38 nm	2.60%	3.70 nm	-3.51%

Table 4: Use of the plano-plano model to predict self-weight deflections of various lens shapes

We can conclude from Table 4:

1. Although these elements are not strongly curved, it is apparent that even minor differences in shape affect the amount of gravity sag significantly.
2. Estimating the amount of central deflection based on a simplified plano-plano case may provide insight but is of limited accuracy.
3. Equation (2) results correlate well with the FEA model.

4. “REAL WORLD” EFFECTS, AS-BUILT

The discussion to this point has centered on the self-weight deflection of an element that is supported uniformly circumferentially around its edge. An analogous mounting method is to support the element with a compliant ring, or to bond the element around its circumference. However, in many cases, it is desirable to allow the element to rest on a hard seat to establish both centration of the optical surface, as well as the axial position of the element⁴. Unless this hard seat has been made kinematic, there may be undesired effects when the element is placed on the seat. A large thin lens, resting on a hard seat, will often distort by beginning to take the shape of the seat. Even very small effects from the machining process can cause an element to be distorted to a higher degree than it would be if placed on a compliant ring.

One example of the quality of metals machining can be observed with lens seats that are not perfectly round. Many materials will “spring” when machined, leaving lens seats that were meant to be perfectly circular slightly elliptical in shape. This effect is generally minute; but, considering that the optical surface contacting the lens seat is almost perfectly spherical, even a seat that is elliptical at the micron level will be enough to ruin the line contact that we expect. In this case, a two-point contact may occur. The situation then arises, where the majority of the element’s weight will be supported on only two points contacting the minor axis of the elliptical lens seat.

Since elements are often mounted in cells, it is likely that two-point contact may be observed in practice. The authors needed to incorporate a fabricated high-precision lens element into a demanding optical assembly. The lens shape was a concave-convex weak meniscus, with concave radius = 487.963 mm, convex radius = 102.447 mm, diameter = 87 mm, clear aperture = 80 mm, center thickness = 13.2 mm, and glass type = Schott N-LAF2. All surfaces were required to meet as-built surface irregularities of $< \lambda/20 = 0.050\lambda = 31.7 \text{ nm}$ (@ $\lambda = 633 \text{ nm}$) P-V departure from ideal spherical shape. In actual use, the concave surface was to face vertically pointing up, so the lens seat was against the downward facing convex side.

To minimize the effects of gravity, the element was initially supported on a seat of 50 mm diameter (which is inside the element's clear aperture). The precision metrology incorporated the use of calibrated interferometry to eliminate the systematic errors of the interferometer,⁵ allowing measurements to a level of $\lambda/100$ to be achievable. All measurements were made with the interferometer's axis oriented vertically (with the test lens' optical axis parallel to gravity). Figure 4 shows the interferometric surface map of the fabricated free-state concave surface to be $0.0226 \lambda = \lambda/44$ over its 80 mm clear aperture.

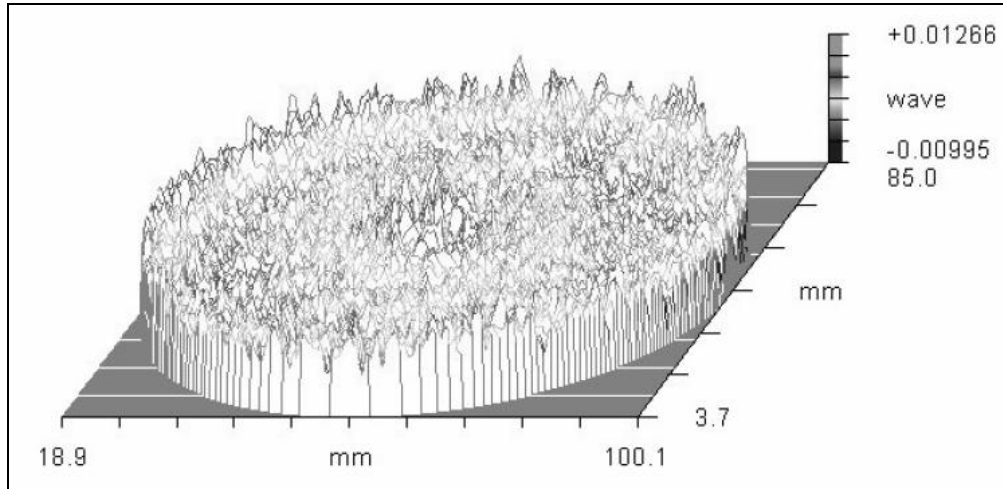


Figure 4: Interferometric surface map of concave surface in free-state

The lens element was subsequently potted into a high-precision stainless steel cell with seat diameter = 81.9 mm. The surfaces of the potted lens subassembly were then tested again. This time we found the optical surfaces to be distorted in a *non-rotationally symmetric* manner greater than the required $\lambda/20$ specification. After thorough investigations to assure that no stresses were being imparted to the lens through the adhesive being used, we eventually discovered that the lens element was already changing its shape asymmetrically when simply placed into the cell vertically, before any adhesive was ever applied.

Figure 5 shows the interferometric surface map of the upward facing concave surface of the fabricated lens element. It was resting under its own weight in its intended metal cell, prior to any adhesives being applied. It exhibited an astigmatic saddle shape of P-V = $0.0771 \lambda = \lambda/13 = 49 \text{ nm}$ over a metrology mask diameter = 77.6 mm.

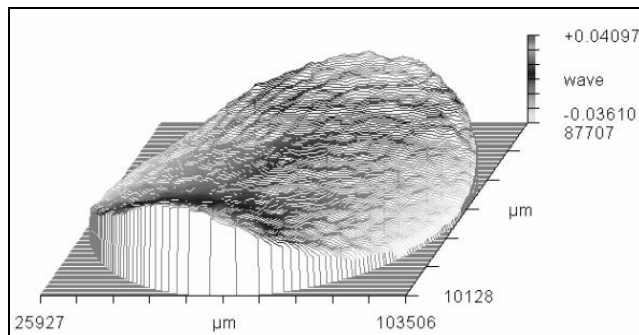


Figure 5: Interferometric surface map of concave surface of lens resting in cell

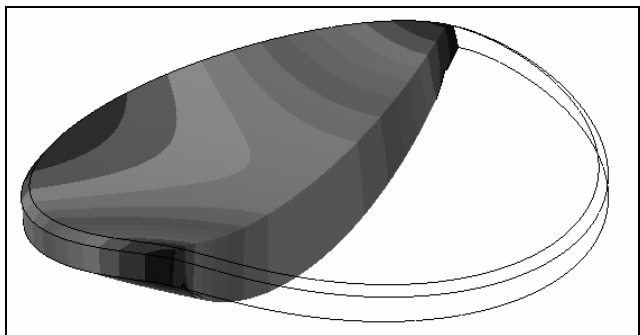


Figure 6: FEA prediction of lens resting in cell with primarily two-point contact

An FEA model of the identical lens element was created to understand the measured data. Figure 6 shows the resulting prediction of the lens in cross section, with contours of departure from the pre-stressed condition overlaid. The lens element was constrained to rest on only two points oriented 180° apart and separated by a distance equal to the seat

diameter of 81.9 mm. The surface showed a similar saddle shape to that of the measured surface of Figure 5. The FEA P-V distortion = $47.5 \text{ nm} = 0.0750\lambda = \lambda/13$ over the same metrology diameter of 77.6 mm, which compared closely with that of the measured data.

Figure 7 is an FEA model created for the same element when resting on a perfectly circular seat. The resulting distortion of the concave surface was P-V = $6.7 \text{ nm} = 0.0101\lambda = \lambda/94$. Thus, the distortion analyzed in Figure 6 with two-point support was approximately seven times greater than the distortion predicted in Figure 7 with a perfectly circular seat.

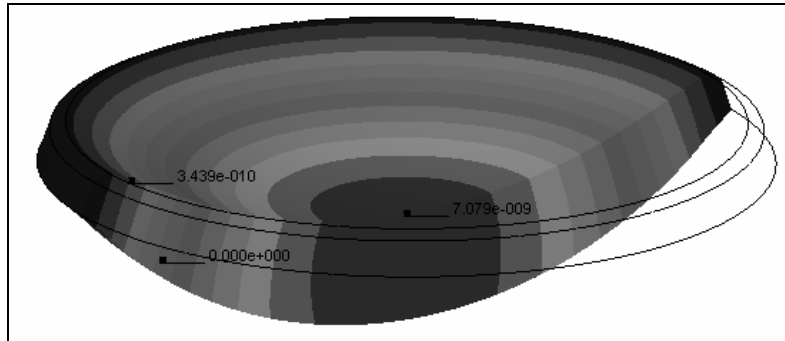


Figure 7: FEA prediction of lens resting on *circular seat*

Through experimentation, we were able to find mounting conditions that were more favorable. The metal cells were turned on a precision lathe yet tended to exhibit elliptical seats at the micron level. With extra care in machining, and by rotating the lens with respect to the cell during assembly, we found cases where the element's weight was distributed uniformly over three points spaced at $\sim 120^\circ$, as shown in Figure 8.

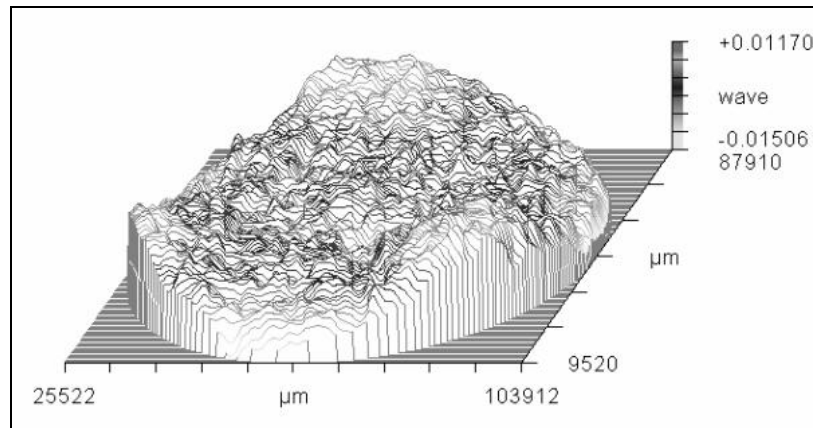


Figure 8: Interferometric surface map of concave surface, convex side resting on primarily three-point contact

This measurement showed a much-improved distortion that was no longer saddle-shaped, but had a traditional trefoil pattern. The measured P-V = $0.0268\lambda = \lambda/37 = 17 \text{ nm}$ at a 78.4 mm aperture. The corresponding FEA model of the element, now supported by three equi-spaced points on the 81.9 mm seat diameter, is shown in Figure 9.

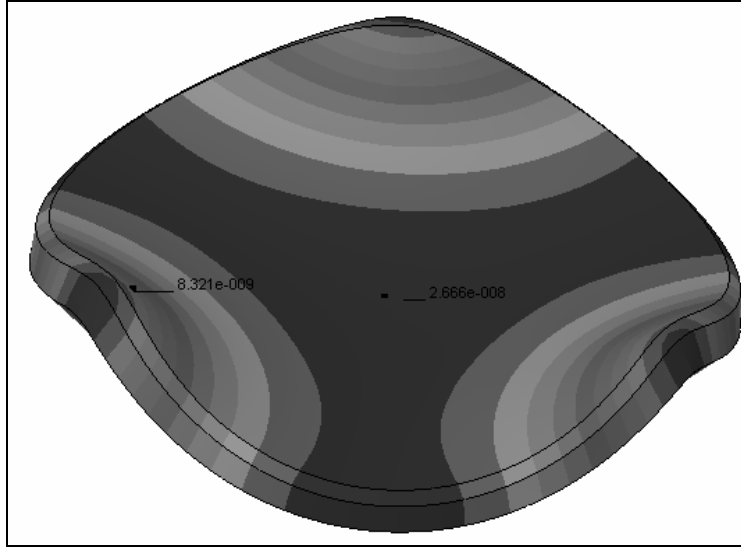


Figure 9: FEA prediction of the element with primarily three-point contact

In this case, the distortion P-V = $0.0290\lambda = \lambda/34 = 18.35$ nm, as calculated within the 78.4 mm metrology aperture used in Figure 8.

In general, an element that is supported on three points, equally spaced around the contact diameter, represents the best possible condition for successful mounting against a hard seat.

We can incorporate the “real-world” learning into our closed-form solution of the minimum thickness required to achieve success. We observed that the worst-case scenario for the placement of a lens on a lens seat occurred when two-point contact is made 180° apart. The induced irregularities of a lens element may be more than seven times those predicted for the self-weight deflection using a perfectly circular seat. By modifying Equation (4), we include a constant factor, S, to be determined empirically, which accounts for the effects of non-ideal mounting seats:

$$t = \sqrt{\frac{3 \cdot S \cdot \rho \cdot g \cdot a^4 (5 + \nu)(1 - \nu)}{16E \cdot |y_c|}} \quad (5)$$

Using Equation (5), we can estimate the thickness required for our N-LAF2 meniscus element to prevent it from distorting by more than $\lambda/20$ when placed on an elliptical seat. To apply Equation (5), the diameter of the lens now was chosen to be equal to that of the seat diameter = 81.9 mm, $S = 7$, and $y_c = \lambda/20 = 31.7$ nm. The resultant minimum required thickness = 15.58 mm, or 2.38 mm (~15%) thicker than the original fabricated element was designed to be.

The FEA analysis depicted in Figure 6 was then repeated for a new element thickness of 15.58mm. The predicted distortion P-V = 31.93 nm = $0.0504\lambda = \lambda/19.8$. Considering our chosen factor $S = 7$ was based on relatively little input data, this result showed a better than expected correlation between the FEA model and the result achieved through application of Equation (5). This level of agreement may not occur for all lens shapes and materials. However, the example serves to illustrate the usefulness of Equation (5) for determining a good estimate of required minimum thickness for lens elements with relatively weak curvatures. Without needing to resort to FEA analysis, preliminary considerations of ideal lens thicknesses can be simply calculated in the early stages of a design.

Table 3 can also be updated to account for the higher distortions caused by elliptical seats. Again, setting $S = 7$, Equation (5) is tabulated below.

Part Diameter (mm)	Maximum Diameter to Thickness Ratio
25	13:1
50	7:1
100	3:1
150	2:1
200	2:1

Table 5: Diameter to thickness ratio required to prevent self-weight distortions in excess of $\lambda/50$, including a 7x factor to account for mounting effects

5. SUMMARY

Table 5 is shown to illustrate the method for choosing appropriate element thicknesses without the need for any calculations whatsoever. However, it was generated with values for Poisson's ratio and Young's modulus appropriate for F5 glass. Greater accuracy for a specific case can be achieved by using the correct material properties for the application. It is also important to determine a value for "S" that is appropriate for the intended mounting conditions. The value may be determined either through analysis or experimentally. In addition, FEA can be used as a further check, once a design form has been identified.

Given the increasing demands placed on allowable surface irregularity, attention must be paid to self-weight deflection of optics and the resulting optical surface distortions. In some cases, it may be appropriate to simulate and analyze the deflection of an optical element as resting on a perfect lens seat. In other cases, the boundary conditions must be adjusted to account for the likely contact points of the optical element on surrounding metals. In cases where the contact is not well distributed, the distortions are not only greater, but also of a more disruptive nature, since they are generally no longer circularly symmetric. The closed-form approximation for plate deflection can be a useful tool for understanding the contribution of the various drivers. Material properties and part dimensions need to be considered. Finite element techniques, coupled with experimentation, are likely to be required when a part's boundary conditions or geometries become more complex.

REFERENCES

-
- ¹ Vukobratovich, Daniel, *Introduction to Opto-Mechanical Design*, Course Notes, 1993
- ² Young, Warren and Budynas, Richard, *Roark's Formulas for Stress and Strain*, McGraw-Hill, 2002
- ³ Yoder, Paul, *Mounting Lenses in Optical Instruments*, SPIE Tutorial Text Vol. TT21, Table B1, SPIE Press Bellingham, 1995
- ⁴ DeWitt IV, Frank and Nadorff, Georg, *Rigid Body Movements of Optical Elements due to Opto-Mechanical Factors*, Proc. SPIE Vol. 5867, San Diego, California, 2005
- ⁵ O'Donohue, S.; Devries, G.; Murphy, P.; Forbes, G.; Dumas, P., *New methods for calibrating systematic errors in interferometric measurements*, Proc. SPIE Vol. 5869, San Diego, CA., 2005